Change Detection in Satellite Images Using a Genetic Algorithm Approach

Turgay Celik

***Abstract*—In this letter, we propose a novel method for unsupervised change detection in multitemporal satellite images by minimizing a cost function using a genetic algorithm (GA). The difference image computed from the multitemporal satellite images is partitioned into two distinct regions, namely, "changed" and "unchanged," according to the binary change detection mask realization from the GA. For each region, the mean square error (MSE) between its difference image values and the average of its difference image values is calculated. The weighted sum of the MSE of the changed and unchanged regions is used as a cost value for the corresponding change detection mask realization. The GA is employed to find the final change detection mask with the minimum cost by evolving the initial realization of the binary change detection mask through generations. The proposed method is able to produce the change detection result on the difference image without *a priori* assumptions. Change detection results are shown on multitemporal Advanced Synthetic Aperture Radar images acquired by the ESA/Envisat satellite and on multitemporal optical images acquired by the Landsat multispectral scanner. The comparisons with the state-of-the-art change detection methods are provided.**

***Index Terms*—Advanced Synthetic Aperture Radar (ASAR) image, change detection, difference image, environmental monitoring, genetic algorithm (GA), log-ratio image, multitemporal satellite images, optical image, remote sensing.**

I. Introduction

CLIMATE change has been widely recognized as one of the major environmental problems. The risen global temperature has brought changes in weather patterns, increased frequency and intensity of extreme weather, and rising sea levels. All these lead to land changes that could automatically be observed through multitemporal satellite images. Automatically addressing the land changes due to climate change is central to the work of unsupervised change detection methods. Unsupervised change detection is a process that makes a direct comparison of a pair of remote sensing images acquired on the same geographical area at different time instances in order to identify changes that may have occurred.

Most of the unsupervised methods are developed based on the analysis of the difference image. The difference image can be formed either by taking the difference of the two images or by computing the logarithm of the two images (log-ratio image). In [1], two automatic techniques based on the Bayes theory for the analysis of the difference image were proposed. The first technique, which is referred to as the expectation-maximization (EM)-based approach, allows an automatic selection of the decision threshold for minimizing the overall change detection error under the assumption that the pixels of the difference image are spatially independent. The second technique, which is referred to as the Markov-random-field (MRF)-based approach, is based on the MRFs and analyzes the difference image by considering the spatial contextual information included in the neighborhood of each pixel. The EM-based approach is free of parameters, whereas the MRF-based approach depends on the parameter β, which influences the spatial contextual information on the change detection process.

Recently, a computationally efficient yet effective method for unsupervised change detection has been proposed in [2], which is referred to as the principal component analysis (PCA)-based approach. The method analyzes the difference image by using the PCA and the k-means clustering algorithm with $k = 2$. The feature vector for each pixel is established by projecting the local change data onto the eigenvector space. The number of eigenvectors determines the dimensionality of the feature vector. The eigenvector space is created by the PCA of $h \times h$ nonoverlapping blocks collected from the entire difference image. The k-means clustering is then employed on the PCA-extracted feature vectors to compute the final change detection result. The method produces promising results with low computational cost. The PCA is employed for dimension reduction and feature extraction, which is a canonical technique to find useful data representations in a space with a much-reduced dimensionality. The PCA can only separate pairwise linear dependencies between data points; because of this reason, PCA-based methods may fail in situations where the dependencies between data points are highly nonlinear. Furthermore, the parameter h is needed to be chosen appropriately.

Transform-domain techniques are applied to reduce the effect of noise contamination and to analyze the difference image using a multiresolution structure. In [3], which is referred to as the multiscale-based approach, the difference image computed in the spatial domain from multitemporal images is decomposed using undecimated discrete wavelet transform (UDWT). Then, for each pixel in the difference image, a multiscale feature vector is extracted using the subbands of the UDWT

Manuscript received July 24, 2009; revised September 3, 2009 and October 12, 2009. Date of publication January 22, 2010; date of current version April 14, 2010. This work was supported by the Singapore Ministry of Education under Grant R-143-000-358-112.

The author is with the Department of Chemistry, Faculty of Science, National University of Singapore, Singapore 117543, and also with the Bioinformatics Institute, Agency for Science, Technology and Research, Singapore 138671 (e-mail: celikturgay@gmail.com; chmcelik@nus.edu.sg).

Digital Object Identifier 10.1109/LGRS.2009.2037024

decomposition and the difference image itself. The final change detection map is obtained by clustering the multiscale feature vectors using the k-means algorithm into two disjoint classes: "changed" and "unchanged." This method, generally speaking, performs quite well, particularly on detecting adequate changes under strong noise contaminations, but it has problems in detecting accurate region boundaries between changed and unchanged regions caused from the direct use of subbands from the UDWT decompositions. In addition, the method depends on the number of scales used in the UDWT decomposition.

All the aforementioned unsupervised change detection methods depend on the parameter tuning or *a priori* assumptions in modeling the difference image data. The parameter tuning process and the *a priori* assumptions in difference image data modeling make them unsuitable for change detection on different types of satellite images. Because of this reason, there is a requirement for a general-purpose unsupervised change detection method which can perform well on different types of satellite images. Recent advances in computing technology make it possible to perform high-load computations very fast by employing parallel computing with high-powered processors. This motivates us to solve the change detection problem by using a genetic algorithm (GA) [4]. The GA is employed to find the final change detection mask by evolving the initial realization of the binary change detection mask through generations. The proposed method is able to produce the change detection result on the difference image without *a priori* assumptions and the parameter tuning process.

This letter is organized as follows. Section II describes the proposed unsupervised change detection method. Section III provides some experimental results of the proposed method and compares with the state-of-the-art methods presented in [1]–[3]. Section IV concludes this letter.

II. Proposed Change Detection Method

Let us consider two images $\mathbf{X}_1 = \{x_1(i,j) | 1 \leq i \leq H, 1 \leq j \leq W\}$ and $\mathbf{X}_2 = \{x_2(i,j) | 1 \leq i \leq H, 1 \leq j \leq W\}$ of size $H \times W$ pixels acquired on the same geographical area but at two different time instances. Let us further assume that such images have been registered with respect to each other [5]. The main objective of this work is to generate a binary change detection mask $\mathbf{CM} = \{cm(i,j) | 1 \leq i \leq H, 1 \leq j \leq W\}$, where $cm(i,j) \in \{0,1\}$, based on the difference image $\mathbf{X}_d$ computed from multitemporal images.

The proposed change detection method is composed of two main parts: 1) image comparison to compute the difference image and 2) generation of the final change detection mask by using the GA on the difference image.

The first step of the proposed method is to generate the difference image using the images $\mathbf{X}_1$ and $\mathbf{X}_2$. Let $\mathbf{X}_d$ be the difference image, which can be computed differently with respect to the type of input image. For the optical images, $\mathbf{X}_d$ can be computed as an absolute-valued difference of the intensity values of two images, i.e.,

$$\mathbf{X}_d = |\mathbf{X}_2 - \mathbf{X}_1|. \tag{1}$$

Meanwhile, when the input satellite images are Advanced Synthetic Aperture Radar (ASAR) images, then $\mathbf{X}_d$ can be computed by the absolute-valued log ratio of $\mathbf{X}_1$ and $\mathbf{X}_2$, i.e.,

$$\mathbf{X}_d = \left| \log \frac{\mathbf{X}_2}{\mathbf{X}_1} \right| = |\log \mathbf{X}_2 - \log \mathbf{X}_1| \tag{2}$$

where log stands for natural logarithm. The pixel values of the difference image $\mathbf{X}_d$ are normalized into [0, 1].

The final change detection mask is computed by segmenting the difference image into the changed and unchanged regions by employing the GA. The change detection mask $\mathbf{CM}$ is a binary datum with $2^{H \times W}$ possible combinations. Each realization of $2^{H \times W}$ possible combinations has a cost which is computed from the difference image $\mathbf{X}_d$. One of the $2^{H \times W}$ possible combinations with the minimum cost can be selected as the optimum $\mathbf{CM}$. An exhaustive way of finding the optimum $\mathbf{CM}$ with the minimum cost is examining all possible $2^{H \times W}$ combinations. It is realistically impossible to examine all possible combinations. Therefore, the GA is employed to find the optimum change detection mask which provides the minimum cost. The difference image $\mathbf{X}_d$ is used together with the GA to find the resultant $\mathbf{CM}$. The GA performs the following steps.

1) Generate the initial population randomly, which consists of K individuals, and set the generation index $g = 1$.
2) Evaluate the cost value (fitness value) of each individual.
3) Select parent individuals randomly.
4) Generate offspring individuals from parent individuals by applying crossover and mutation.
5) Evaluate the cost value (fitness value) of all offspring individuals.
6) Select individuals to be transferred to the next generation through the elite transferring strategy and tournament rule.
7) Return selected individuals to the population.
8) Set $g = g + 1$, and return to step 3), where g is the generation index and K is the total number of individuals in the population at each generation.

In the GA, each population consists of a fixed number of individuals which are $H \times W$ binary change detection mask realizations generated by the GA. In each generation, two individuals are randomly selected from the population, and multiple offsprings are produced based on them. Among the individuals and offsprings, the most adaptive individual and the individual that is selected according to tournament selection are returned to the original population. The most optimal individual is searched by repeating this process.

Each individual in a generation has a cost value (fitness value). Let $\mathbf{C}_k^g$ be individual k, $k = 1, \ldots, K$, at generation g and F_k^g be the corresponding cost value (fitness value). The cost value (fitness value) F_k^g is computed using $\mathbf{X}_d$ and $\mathbf{C}_k^g$ as follows:

$$F_k^g = \sum_{r=0}^{1} \frac{N_r}{H \times W} \sum_{\forall (i,j) \in \mathbf{R}_r} (\mathbf{X}_d(i,j) - \mu_r)^2 \tag{3}$$

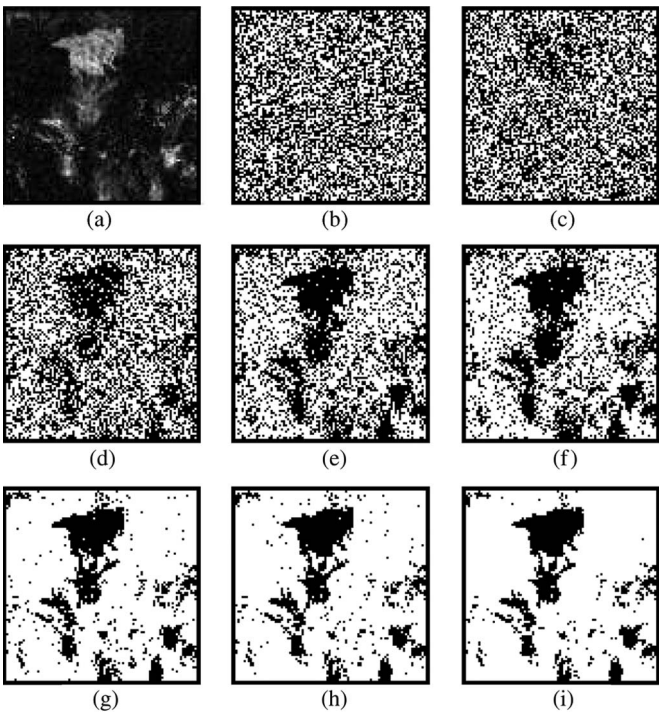

Fig. 1. Intermediate change detection masks with the minimum cost according to (3) ($\mathbf{C}^g$) obtained by the proposed method at different generations (g) on the difference image. (a) Difference image ($\mathbf{X}_d$). (b) $\mathbf{C}^1$. (c) $\mathbf{C}^{100}$. (d) $\mathbf{C}^{1000}$. (e) $\mathbf{C}^{5000}$. (f) $\mathbf{C}^{10\,000}$. (g) $\mathbf{C}^{100\,000}$. (h) $\mathbf{C}^{150\,000}$. (i) Resultant change detection mask ($\mathbf{C}^{200\,000}$).

where $\mathbf{R}_0$ and $\mathbf{R}_1$ denote all changed pixels, i.e., $\mathbf{R}_0 = \{(i, j)|c_k^g(i, j) = 0\}$, and unchanged pixels, i.e., $\mathbf{R}_1 = \{(i, j)|c_k^g(i, j) = 1\}$, respectively, and N_0, N_1, μ_0, and μ_1 are defined as follows:

$$N_0 = \sum_{\forall (i,j) \in \mathbf{R}_0} 1 \qquad N_1 = \sum_{\forall (i,j) \in \mathbf{R}_1} 1$$

$$\mu_0 = \frac{1}{N_0} \sum_{\forall (i,j) \in \mathbf{R}_0} \mathbf{X}_d(i, j) \qquad \mu_1 = \frac{1}{N_1} \sum_{\forall (i,j) \in \mathbf{R}_1} \mathbf{X}_d(i, j).$$

In the aforementioned cost value (fitness value) equation, for each region ($\mathbf{R}_r$), the mean square error (MSE) between its difference image values ($\mathbf{X}_d(i, j)\ \forall (i, j) \in \mathbf{R}_r$) and the average of its difference image values (μ_r) is calculated. The weighted sum of the MSE of the changed and unchanged regions is used as a cost value for the corresponding change detection mask realization. The lower the MSE, the better the partition is. Equation (3) approaches to zero when $\mathbf{C}_k^g$ partitions the difference image $\mathbf{X}_d$ into changed and unchanged regions adequately, and vice versa.

The intermediate change detection masks produced by the proposed method on the difference image shown in Fig. 1(a) are shown in Fig. 1. The algorithm starts by randomly producing an initial change detection mask, as shown in Fig. 1(b). The initial change detection mask is iteratively refined according to the cost function in (3) to obtain the final change detection mask [see Fig. 1(b)–(i)].

III. Experimental Results

A. Description of Data Sets

In order to assess the effectiveness of the different change detection techniques for the analysis of the difference image, we considered real multitemporal data sets corresponding to the geographical area of the flooding in Bangladesh and parts of India brought on by two weeks of persistent rain, and a forest fire on the Reno–Lake Tahoe area of Nevada.

The ASAR multitemporal images collected by ESA/Envisat on Bangladesh and parts of India are used in the experiments. ASAR, which is able to peer through clouds, rain, or local darkness, records the signal backscattered by the Earth's land, sea, and ice surfaces. The backscattering measure recorded by the sensor from water is very different from land and vegetation, making comparing before and after images very effective for locating flooded regions.

The first data set is available from [6], which contains a large set of ASAR images. Two of them are chosen for our simulation experiments and shown in Fig. 2, which are acquired on April 12, 2007 [see Fig. 2(a)], and July 26, 2007 [see Fig. 2(b)], by the ESA/Envisat satellite. A small area with 300×300 pixels each indicated by the white rectangles in Fig. 2(a) and (b) is enlarged and shown in Fig. 2(c) and (d), respectively. The ground truth of the change detection mask for the flooding area, which is shown in Fig. 2(e), was created by a manual analysis of the input images based on Fig. 2(c) and (d).

The second data set is available from [7], which contains optical images. The images of size 200 × 200 pixels are acquired on August 5, 1986 [see Fig. 2(f)], and August 5, 1992 [see Fig. 2(g)], by the Landsat Multispectral Scanner (MSS) to observe the land deformations on the Reno–Lake Tahoe area of Nevada resulted from a forest fire. The ground truth of the change detection mask for the forest fire area, which is shown in Fig. 2(h), was created by a manual analysis of the input images based on Fig. 2(f) and (g).

B. Quantitative Measures

We perform qualitative and quantitative experiments on the data sets. In order to perform the quantitative experiments, the input test images, together with their ground truth change detection masks, are used. Once the binary change detection mask has been obtained by using the change detection method, the following defined quantities are computed for comparing the computed change detection mask against the ground truth change detection mask.

1) *False alarms* (FA): The number of unchanged pixels that were incorrectly detected as changed, and the false alarm rate in percentage $P_{FA} = FA/N_1 \times 100$.
2) *Missed alarms* (MA): The number of changed pixels that were incorrectly detected as unchanged, and the missed alarm rate in percentage $P_{MA} = MA/N_0 \times 100$.
3) *Total errors* (TE): The sum of false alarms (FA) and missed alarms (MA), and the total error rate in percentage $P_{TE} = (FA + MA)/(N_0 + N_1) \times 100$, where N_0 and N_1 are the total number of changed and

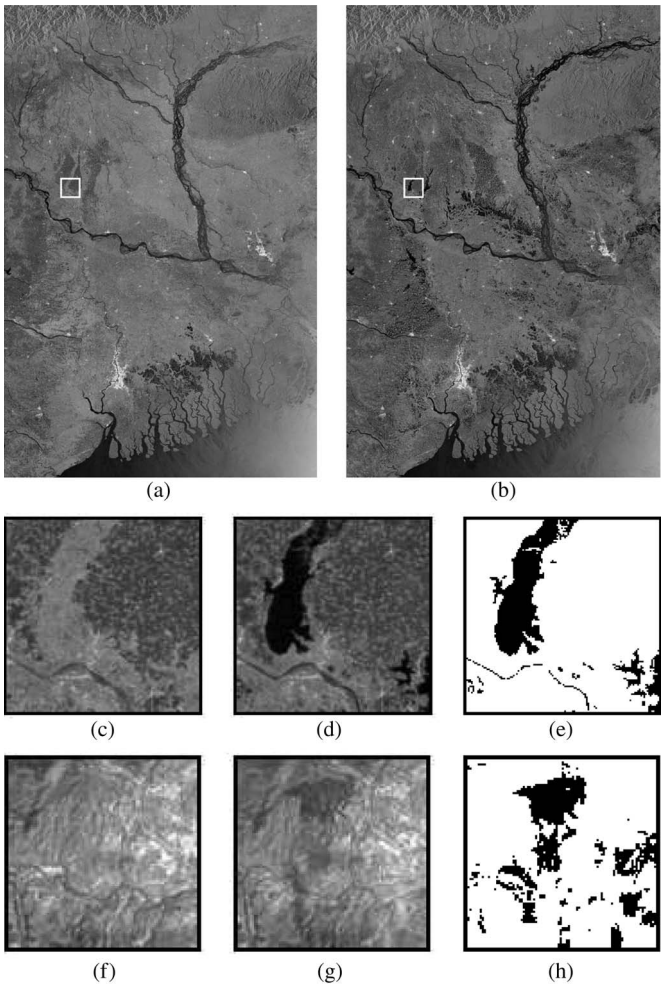

Fig. 2. Data sets used in the experiments. (a) ESA/Envisat ASAR image acquired on April 12, 2007. (b) ESA/Envisat ASAR image acquired on July 26, 2007. (c) Enlargement of the white area in (a). (d) Enlargement of the white area in (b). (e) Ground truth of the change detection mask between (c) and (d). (f) Landsat MSS image acquired on August 5, 1986. (g) Landsat MSS image acquired on August 5, 1992. (h) Ground truth of the change detection mask between (f) and (g).

unchanged pixels in the ground truth change detection mask, respectively.

C. Experiments

In GA implementation, each population consists of 20 individuals; hence, $K = 20$, and a two-point uniform crossover with crossover rate $\mathrm{P}_C = 0.8$ is used together with a uniform mutation of rate $\mathrm{P}_M = 0.01$ to evolve the initial population through generations. We compare the proposed method with the change detection methods [1]–[3] from the literature which perform an unsupervised change detection task with minimal parameter tuning. The techniques in [2] and [3] have been recently developed, and they provide promising results regardless to the types of input satellite images. The change detection methods presented in [1]–[3] are implemented using the same set of default parameters given in those papers.

The quantitative and qualitative change detection results obtained from different methods for input ASAR images shown in Fig. 2(c) and (d) are tabulated in Table I and shown in Fig. 3, respectively. The proposed method achieves 1.82% total error rate and, hence, 98.18% correct detection rate. The PCA-based approach [2] and the multiscale-based approach [3] provide very similar performance results with 3% performance degradation on the average with respect to the proposed approach. Meanwhile, the change detection results from the EM-based approach [1] and the MRF-based approach [1] show 17% performance degradation on the average with respect to the proposed method. The change detection results from the EM-based approach [1] and the MRF-based approach [1] are very noisy. This is mainly due to the fact that the unimodal Gaussian model employed in modeling the difference image data fails to provide accurate data modeling.

TABLE I
FALSE ALARMS, MISSED ALARMS, AND TOTAL ERRORS (IN NUMBER OF PIXELS AND PERCENTAGE) RESULTED FROM DIFFERENT CHANGE DETECTION METHODS ON ASAR TEST IMAGES

Change detection method	False Alarms		Missed Alarms		Total Errors	
	Pixels	P_{FA}	Pixels	P_{MA}	Pixels	P_{TE}
EM-based approach [1]	16885	23.16	0	0.00	16885	18.76
MRF-based approach [1]	16720	22.93	0	0.00	16720	18.58
PCA-based approach [2]	129	0.18	3719	21.77	3848	4.28
Multiscale-based approach [3]	300	0.41	3874	22.68	4174	4.64
Proposed	661	0.91	976	5.71	1637	1.82

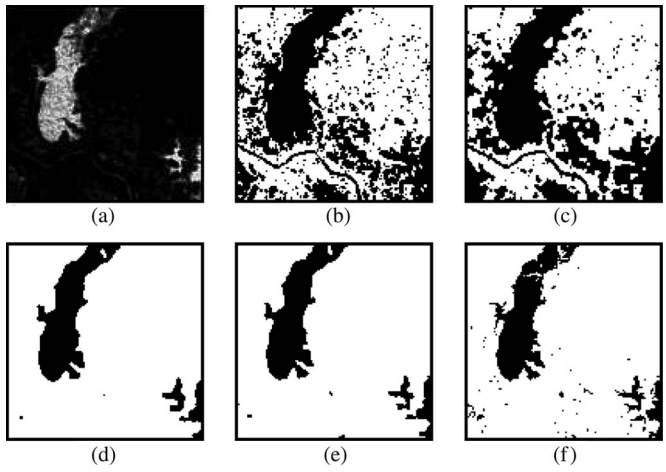

Fig. 3. Qualitative change detection results by using different change detection methods on ASAR test images as shown in Fig. 2(c) and (d). (a) Difference image ($\mathbf{X}_d$). (b) EM-based approach [1]. (c) MRF-based approach [1]. (d) PCA-based approach [2]. (e) Multiscale-based approach [3]. (f) Proposed method.

The qualitative and quantitative test results on the optical image data set acquired by the Landsat MSS are shown in Fig. 4 and tabulated in Table II. Similar to the performance results on the ASAR image data set, it is clear from Fig. 4 and Table II that the proposed change detection method yields the lowest total error rate. Meanwhile, the other change detection methods [1]–[3] show 2% performance degradations on the average with respect to the proposed method when the total error rate is considered. The performance improvements in the EM-based and MRF-based approaches [1] are apparent. This is mainly due to the reason that the data distributions of the changed and unchanged pixels in the difference image computed from

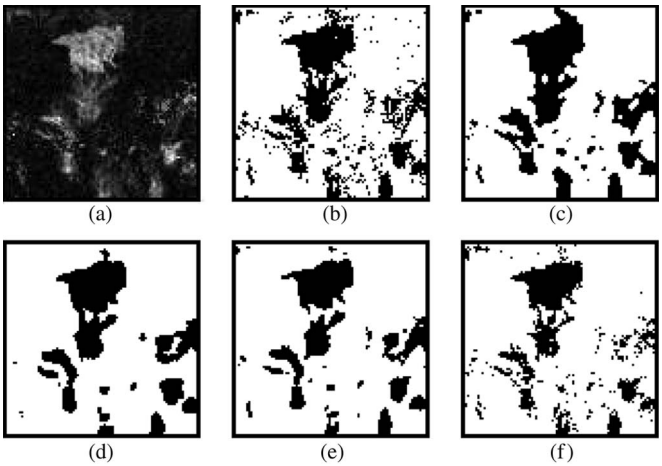

Fig. 4. Qualitative change detection results by using different change detection methods on optical test images as shown in Fig. 2(f) and (g). (a) Difference image. (b) EM-based approach [1]. (c) MRF-based approach [1]. (d) PCA-based approach [2]. (e) Multiscale-based approach [3]. (f) Proposed method.

TABLE II
FALSE ALARMS, MISSED ALARMS, AND TOTAL ERRORS (IN NUMBER OF PIXELS AND PERCENTAGE) RESULTED FROM DIFFERENT CHANGE DETECTION METHODS ON OPTICAL TEST IMAGES

Change detection method	False Alarms		Missed Alarms		Total Errors	
	Pixels	P_{FA}	Pixels	P_{MA}	Pixels	P_{TE}
EM-based approach [1]	5121	7.37	639	3.12	5760	6.40
MRF-based approach [1]	4608	6.63	495	2.42	5103	5.67
PCA-based approach [2]	3330	4.79	1980	9.67	5310	5.90
Multiscale-based approach [3]	2511	3.61	2493	12.17	5004	5.56
Proposed	1485	2.14	2151	10.50	3636	4.04

the optical images are adequately modeled with the unimodal Gaussian distribution.

It is clear from the qualitative and quantitative results on the ASAR and optical test images that the proposed method obtains the change detection mask more accurately than the other techniques [1]–[3] at the expense of higher computational cost. This is mainly because of the directed search carried out by the GA over the subset of all possible combinations of change detection masks and selecting the one with the minimum cost according to the proposed cost function defined in (3). The computation time of the proposed method depends on the size of the input images. For example, the input images shown in Fig. 2(c) and (d) are 300×300 multitemporal images of the same scene; hence, there are $2^{300\times300} \cong 10^{90\,000}$ possible combinations for the change detection mask. The proposed method finds the resultant change detection mask within 200 000 generations. Thus, the total number of change detection masks searched for finding the resultant change detection mask with the minimum cost value is less than $20 \times 200\,000 = 4\,000\,000 = 4 \times 10^6 \ll 10^{90\,000}$. Hence, the GA makes it possible to realize the proposed unsupervised change detection method. We implemented the proposed change detection method in MATLAB on a personal computer with 2-GHz Intel Core2 Duo CPU and 2-GB RAM. For input images of size 300×300 pixels, the proposed method takes 2 h to produce the resultant change detection mask. The total computation time can dramatically be reduced by employing parallel computing techniques.

The cost function defined in (3) does not consider the spatial contextual information included in the neighborhood of each pixel; meanwhile, the MRF-based approach [1], the PCA-based approach [2], and the multiscale-based approach [3] improve their performance by employing the spatial contextual information. The performance of the proposed method can further be improved by considering the spatial contextual information. This can be achieved by modifying the cost function in (3) by considering the neighborhood of each pixel in the difference image. Each pixel's difference image value, for example, can be replaced with an average of the difference image values around that pixel to embed the spatial contextual information into the cost function in (3).

IV. CONCLUSION

In this letter, we have proposed an unsupervised change detection method by minimizing a cost function via a GA. The proposed MSE-based cost function is evaluated for each different realization of the change detection mask produced by the GA. The realization with the minimum cost is evolved through generations of the GA to produce the resultant change detection mask.

Extensive qualitative and quantitative simulation results show that the proposed method consistently performs quite well on both ASAR and optical images. It can automatically handle high variations in the changed and unchanged pixel values of the difference image in producing the change detection mask. This makes it to be applicable for unsupervised change detection in different types of satellite images. Further improvement in the change detection performance can be achieved by considering the spatial contextual information included in the neighborhood of each pixel.

The proposed method has verified that the unsupervised change detection in satellite images without any parameters and *a priori* assumptions in modeling the difference image data is possible by using the GA with a proper cost function. The proposed framework with different cost functions can be employed in complex change detection tasks at the expense of computational cost. The current technology in parallel computing with high-power processors makes the proposed method feasible for unsupervised change detection purposes.

REFERENCES

[1] L. Bruzzone and D. Prieto, "Automatic analysis of the difference image for unsupervised change detection," *IEEE Trans. Geosci. Remote Sens.*, vol. 38, no. 3, pp. 1171–1182, May 2000.
[2] T. Celik, "Unsupervised change detection in satellite images using principal component analysis and k-means clustering," *IEEE Geosci. Remote Sens. Lett.*, vol. 6, no. 4, pp. 772–776, Oct. 2009.
[3] T. Celik, "Multiscale change detection in multitemporal satellite images," *IEEE Geosci. Remote Sens. Lett.*, vol. 6, no. 4, pp. 820–824, Oct. 2009.
[4] J. R. Koza, *Genetic Programming*. Cambridge, MA: MIT Press, 1992.
[5] S. Leprince, S. Barbot, F. Ayoub, and J.-P. Avouac, "Automatic and precise orthorectification, coregistration, and subpixel correlation of satellite images, application to ground deformation measurements," *IEEE Trans. Geosci. Remote Sens.*, vol. 45, no. 6, pp. 1529–1558, Jun. 2007.
[6] Retrieved September 2009. [Online]. Available: http://earth.esa.int/cgi-bin/satimgsql.pl?show_url=1738&startframe=0
[7] Retrieved September 2009. [Online]. Available: http://geochange.er.usgs.gov/sw/changes/natural/reno-tahoe/burn.html